Calhoun

Institutional Archive of the Naval Postgraduate School

Calhoun: The NPS Institutional Archive

Faculty and Researcher Publications   Faculty and Researcher Publications

2013

Statistical Analysis of Touchdown Error for Self-Guided Aerial Payload Delivery Systems

Yakimenko, O.A.

Monterey, California: Naval Postgraduate School

þÿ[P A T C A D] Y a k i m e n k o , O . A . ,   S t a t i s t i c a l A n a l y s i s o f T o u c h d o w n E r r o r f o r

Statistical Analysis of Touchdown Error for Self-Guided Aerial Payload Delivery Systems

Oleg Yakimenko[*]
Naval Postgraduate School, Monterey, CA 93943-5107

   The paper overviews the distributions of touchdown error for a variety of different-weight self-guided parafoil-based payload delivery systems as demonstrated at several Precision Airdrop Technology and Demonstration (PATCAD) events in Yuma, AZ within the period of 2001-2009. The paper aims at establishing the correct procedure to estimate an accuracy of an aerial payload delivery system and also looking at the effect that a guidance law might have on a touchdown error distribution. These approaches and estimates should help a tester community in preparation for the aerodynamic deceleration system (ADS) tests and analysis of their results.

I.   Background

THe Safety Fans Graphical User Interface (GUI)[1,2] was developed to assist test planning officers in organizing and executing developmental and operational tests and evaluations (DT&E and OT&E).[3] Based on just a few characteristics of the aerodynamic decelerator system (number of stages, descent rate, weight, glide ratio, time to deploy canopy) and utilizing the best known winds aloft this allows computing a footprint of the possible touchdown points depending on the release conditions (altitude and speed vector). For self-guided parachute (parafoil) systems characterized by a high glide ratio the upper bound of fly-away distance in the wind coordinate frame can be obtained by simply multiplying a release altitude by the glide ratio. For example, if a system with a glide ratio of 3:1 is released from 3km altitude above a drop zone, it may fly as far as 9km horizontally while it descends. This simplified approach would result in a very large footprint drastically limiting the number of the possible test sites and increasing recourses required to conduct such a test. In practice however, a self-guided ADS try to steer towards an intended point of impact (IPI) exhibiting miss distances of the order of up to only several hundred meters. Therefore, in determining the size of a safety fan for DT and OT we should also rely on a some kind of a measure of goodness of the guidance, navigation and control (GNC) algorithms onboard self-guided ADSs.

   In the military science of ballistics, the circular error probable (CEP) (also circular error probability or circle of equal probability) is used as an intuitive measure of a weapon system's precision.[4] For the guided systems it is defined as the radius of a circle, centered about the IPI (aim point), whose boundary is expected to include 50% of the population within it. The key word in the definition is population, not sample. The CEP may not contain exactly 50% of the sample data points, but it is expected to include 50% of the "true" population. That is why it is important to employ and properly use the appropriate statistical tools.

   The original concept of CEP was based on the circular normal distribution (CND) with CEP as a parameter of the CND just as the mean, μ, and standard deviation, σ, are parameters of the normal distribution. The derivation of CEP for CND starts with the bivariate normal distribution (BND), the statistical distribution with a probability density function (Fig.1)

$$p(x,y) = \frac{1}{2\pi\sigma_x\sigma_y\sqrt{1-\rho^2}} e^{-\frac{z}{2(1-\rho^2)}}$$

(1)

where z is the so-called z-score

$$z = \frac{(x-\mu_x)^2}{\sigma_x^2} - \frac{2\rho(x-\mu_x)(y-\mu_y)}{\sigma_x\sigma_y} + \frac{(y-\mu_y)^2}{\sigma_y^2}$$

(2)

and ρ is the correlation coefficient

[*]Professor, Department of Systems Engineering, Code SE/Yk, oayakime@nps.edu, Associate Fellow AIAA.

$$\rho = cor(x, y) = \frac{\text{cov}(x, y)}{\sigma_x \sigma_y} = \frac{\sum_{i=1}^{n}(x_i - \mu_x)(y_i - \mu_y)}{\sqrt{\sum_{i=1}^{n}(x_i - \mu_x)^2 \sum_{i=1}^{n}(y_i - \mu_y)^2}} \tag{3}$$
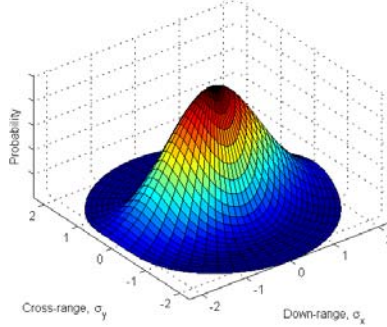

Fig. 1. Bivariate normal distribution.

If $\sigma_x \approx \sigma_y = \sigma$, there is no bias ($\mu_x = \mu_y = 0$) and x-y data are not correlated ($\rho = 0$) then BND becomes CND or Rayleigh distribution with a probability density function

$$p(r) = p(x, y) = \frac{1}{2\pi\sigma^2} e^{-\frac{x^2 + y^2}{2\sigma^2}} = \frac{1}{2\pi\sigma^2} e^{-\frac{r^2}{2\sigma^2}} \tag{4}$$

Using this distribution, the probability of radius r being less than some value a is computed as

$$P(r \le a) = \int_0^a 2\pi r p(r) dr = \frac{1}{2\pi\sigma^2} \int_0^a 2\pi r e^{-\frac{r^2}{2\sigma^2}} dr = 1 - e^{-\frac{a^2}{2\sigma^2}} \tag{5}$$

The CEP is the radius obtained using the above equation for a probability P of 0.5

$$P(r \le CEP) = 0.5 = 1 - e^{-\frac{CEP^2}{2\sigma^2}} \tag{6}$$

or solving for CEP

$$CEP = \sqrt{2\ln 2}\,\sigma \approx 1.1774\sigma \tag{7}$$

If CEP is n meters, 50% of rounds (if we are talking about ballistics) land within n meters of IPI, 43% between n and $2n$, and 7% between $2n$ and $3n$ meters, and the proportion of rounds that lands farther than three times the CEP from IPI is less than 0.2%.

To determine if we are sampling from a CND, the following assumptions must be tested:
- The x and y components of the miss distance are statistically independent ($\rho = 0$)
- The distributions of x and y are both normal
- The distribution is circular ($\sigma_x = \sigma_y$)
- The mean point of impact (MPI) is at IPI ($\mu_x = \mu_y = 0$)

These assumptions are to be verified with a series of tests as shown in Table 1.

Table 1. Parametric and non parametric tests for CEP computation.

	Parametric Test (normal distribution)	Non-Parametric Test (distribution free)
Assumption 1: The x and y components are statistically independent	t-test[5]	Spearman's rho test[6]
Assumption 2: The distributions of x and y are both normal	Chi square test[5]	Lilliefors test[7*]
Assumption 3: The distribution is circular	F-test[5]	Siegel–Tukey test[6]
Assumption 4: The MPI is at IPI	t-test[5]	Wilcoxon signed-rank test[5,9]

*Lilliefors test is used to test whether data come from a normally distributed population without specifying the expected value and variance of the distribution.

However in practice, these assumptions are seldom tested because if they were, you would find the use of CEP to be inappropriate. Specifically, precision-guided munitions generally have more "close misses" and therefore are not normally distributed. Munitions may also have larger standard deviation of range errors than the standard deviation of azimuth (deflection) errors, resulting in an elliptical confidence region. Finally, munition samples may not be exactly on target, that is, the mean vector is not a zero vector ($\mu_x = \mu_y = 0$), but rather biased. For the latter two cases, approximate formulas are available to convert the distributions along the two axes into the equivalent circle radius for the specified percentage.

The paper aims at applying the aforementioned formal methodology of CEP estimation to analyze an accuracy of self-guided ADSs that would allow computing a more realistic size of a safety fan for DT and OT accounting for a maturity of the system and other factors. The paper is organized as follows. Section II lays out a detailed procedure for statistically correct estimation of CEP and reveals some features associated with ADS as opposed to ballistic systems. Section III utilizes the methodology developed in Section II to look at the results of several major ADS demonstrations that occurred during the last decade with the goal of establishing the overall trends in reducing CEP of self-guided ADSs. Section IV employs the same methodology to look at some typical representatives of different-weight ADSs with the same goal of establishing general trends and understanding the reasons causing the difference between CEP estimates for different same-weight class ADSs. Section V discusses the nature and distribution of outliers. The paper ends with conclusion and two addendums dedicated to deriving some bulky relations used in Section II.

II. Example of ADS's Touchdown Accuracy Analysis

Formally, the procedure for CEP estimation looks as follows:
- Gather x and y data pairs (by gathering just the values of radial miss distance we may be loosing a lot of useful information)
- Eliminate obvious outliers
- Test the x and y data sets for normality
- Test for x - y data sets correlation and rotate original data if necessary
- Test whether MPI is at IPI, i.e. compute a bias, and check whether this bias is statistically significant
- Test whether the distribution is circular and compute CEP_{MPI} with respect to MPI
- If the bias happens to be statistically significant, calculate CEP_{DMPI}, i.e. CEP with respect to the desired MPI (DMPI)
- Calculate the upper confidence level for CEP_{MPI} (CEP_{DMPI})

The concept of CEP_{MPI} versus CEP_{DMPI} is illustrated in Figs.2a,b. CEP_{DMPI} has such a value that it encompasses 50% of data (Fig.2c).

There is no analytical solution for CEP_{DMPI}, so its computation is based on a simple expression

$$CEP_{DMPI} = CEP_{MPI} k_{Bias} \tag{8}$$

where the coefficient k_{Bias} represents a numerical approximation. The discussion on how to find this coefficient is given in Addendum A, but for self-guided parafoil-based payload delivery systems featuring $V = \dfrac{Bias}{CEP_{MPI}} < 0.5$ the following quadratic regression can be used:
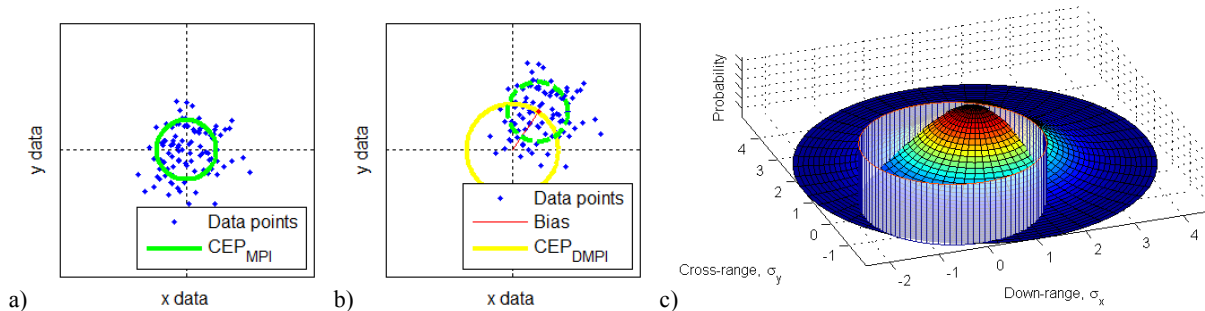
$$k_{Bias} = 0.3525V^2 - 0.00146V + 1 \tag{9}$$

Fig. 2. CEP_{MPI} (a) versus CEP_{DMPI} (b); graphical illustration of CEP_{DMPI} corresponding to Fig.2b (c).

As seen from Fig.3, even in the case of a statistically significant bias accounting for it does not change the computed CEP much – at most it can increase it by about 8%, but for mature ADSs $k_{Bias} \sim 1$ and $CEP_{DMPI} \sim CEP_{MPI}$.
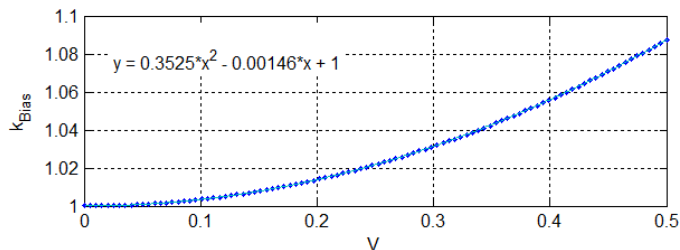

Fig. 3. Coefficient $k_{Bias} = k_{Bias}(V)$ to determine CEP$_{DMPI}$ from CEP$_{MPI}$.

To demonstrate how the CEP estimation routine outlined in the beginning of this section works, Fig.4 features some real drop test data and their preliminary analysis. Specifically, we start from producing a non-parametric box plot (upper-right portion of the figure) revealing several outliers out of the total of 19 data points.
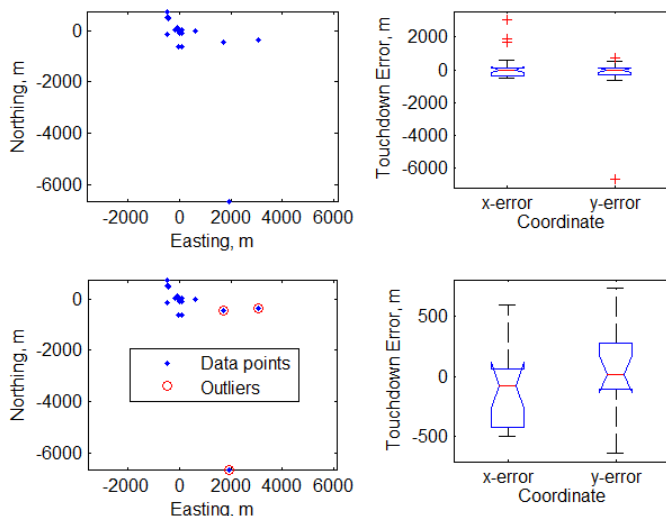

Fig. 4. Non-parametric data conditioning.

By construction, a box plot (aka a box-and-whisker diagram or plot) in Fig.4 graphically depicts numerical data (without making any assumptions of the underlying statistical distribution) through their five-number summaries: the box itself is composed of the lower quartile (Q1), median (Q2), and upper quartile (Q3), while the ends of the whiskers in this case represent ±1.5 interquartile range (IQR=Q3-Q1) above Q3 and below Q1. What appears beyond the whiskers maybe treated as outliers.

As seen from Fig.4 in our specific case we have three obvious outliers, probably caused by structural malfunction (ripped off or twisted control lines) or GNC algorithm not working properly (that may also include an effect of improper mitigation of unknown winds or unmodeled dynamics). Eliminating these three outliers as shown in the bottom-left portion of the figure (leaving n=16 data points to work with) leads to the box plots covering (explaining statistically) all the remaining data (compare the upper-right and bottom-right plots in Fig.4 corresponding to taking into account all 19 and just 16 data points).

It should be noted that in other cases eliminating outliers may not be so straightforward. Consider Fig.5 that represents the relationship between the box plot constructed as described above for the standard normal distribution with a well known bell-shape probability density function for this distribution. As seen for the normal distribution the box plot would cover $[-2.698\sigma; 2.698\sigma]$ range or about 99.3% of the set (compared to about 99.7% for the $[-3\sigma; 3\sigma]$ range. That means that even for the normal distribution we may expect to see about 1% of data points beyond the whiskers that are not necessarily outliers (i.e. cannot be eliminated from the further analysis). For the data points not necessarily distributed normally this amount may be much larger.

According to Table 1 the following procedure rely on population distribution, therefore the normality test needs to be conducted. For example, the Kolmogorov-Smirnov normality test[5] (Fig.6) compares the empirical cumulative distribution function of sample data with the distribution expected if the data were normal. The outcome of this test

is the *p*-value - a small *p*-value is an indication that the null hypothesis (that the observations follow a normal distribution) is false (that is what $p < 0.01$ in Fig.6 stands for). As seen from Fig.6, elimination of three outliers at the previous step allows increasing the *p*-value for both *x* and *y* data sets to the level where the null hypothesis cannot be rejected (to $p > 0.15$ and $p > 0.106$, respectively), so we may assume that the data points are distributed normally.
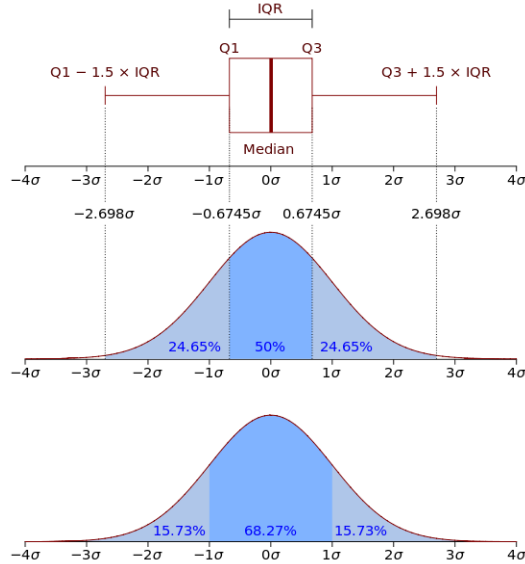

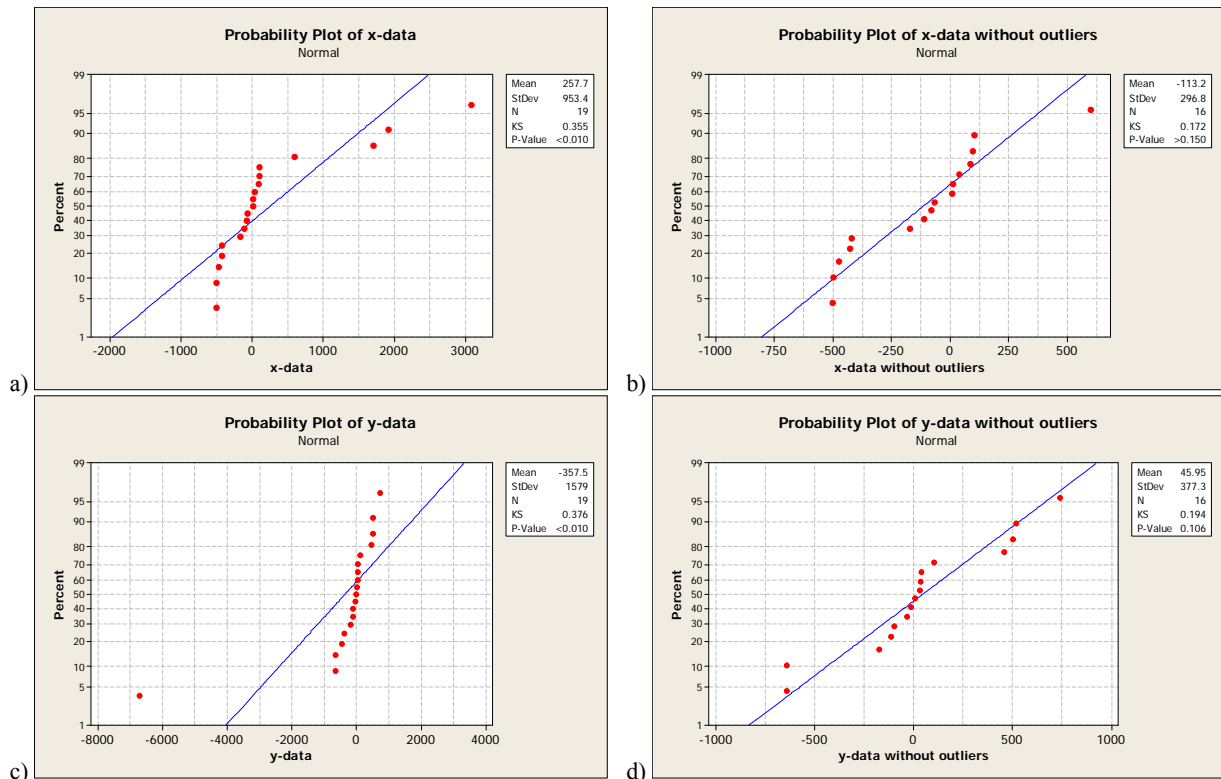Fig. 5. Explanation of the box plot concept as applied to the normal distribution.

Fig. 6. Normality test for the original (a, c) and reduced (b, d) data sets.

Next, the correlation analysis to reveal a possible correlation between *x* (Northing) and *y* (Easting) data takes place. The correlation coefficient ρ defined in (3) is used in the *t* test with the *t*-statistic computed as

$$t_s = \frac{|\rho|\sqrt{n-2}}{\sqrt{1-\rho^2}} \tag{10}$$

This value is then compared with the critical value of *t*-statistic (a ratio of the departure of an estimated parameter from its notional value and its standard error). In our case (for $n = 16$) $\rho = -0.56$, which leads to $t_s = 2.54$. This value happens to be larger than the critical value $t_{0.02,14} = 2.26$ (here 0.02 stands for 98%=100(1-0.02)% confidence level and 14=*n*-2 defines the number of degrees of freedom (DF)). This means that in our specific case the correlation happens to be significant (which for instance might be caused by the NW direction of the prevailing surface winds during the tests); hence the data set needs to be rotated by some angle computed as

$$\theta = \frac{1}{2}\arctan\left(\frac{2\rho\sigma_x\sigma_y}{\sigma_x^2 - \sigma_y^2}\right) \tag{11}$$

so that the data point coordinates in the new coordinate frame become

$$\begin{pmatrix} u \\ v \end{pmatrix} = R_\theta \begin{pmatrix} x \\ y \end{pmatrix} = \begin{pmatrix} \cos\theta & \sin\theta \\ -\sin\theta & \cos\theta \end{pmatrix} \begin{pmatrix} x \\ y \end{pmatrix} \tag{12}$$
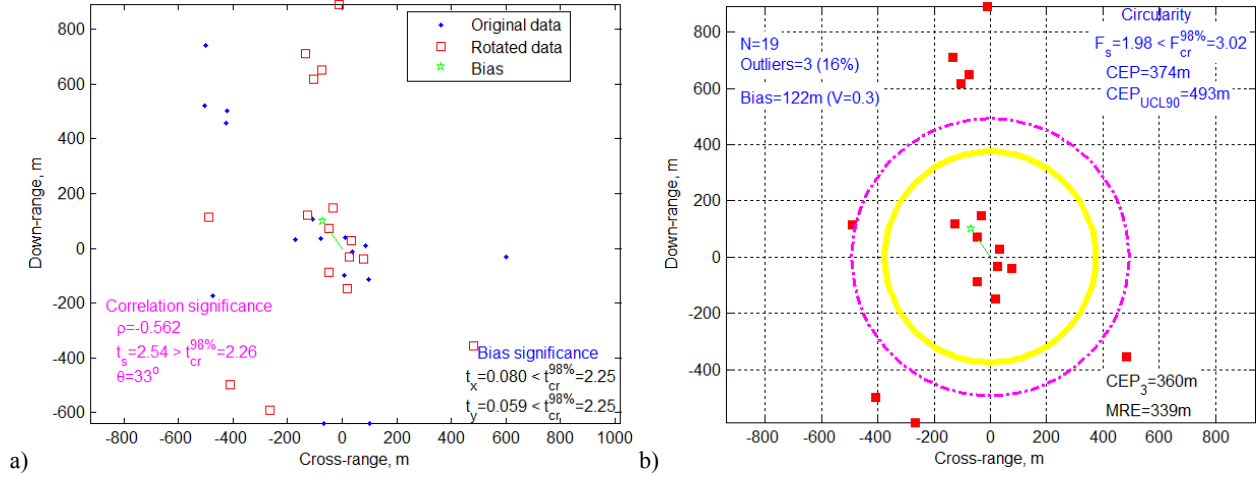
In our case $\theta = 33°$ (Fig.7a).

Fig. 7. Data rotation (a); and CEP$_{MPI}$ (b) calculation.

The next step is to evaluate a statistical significance of the bias (which in our case happens to be 122m). We do it by comparing the critical value of $t_{0.02,15} = 2.25$ with the values of corresponding *u* and *v* statistics

$$t_u = \frac{\bar{u}}{s_u/\sqrt{n}} \text{ and } t_v = \frac{\bar{v}}{s_v/\sqrt{n}} \tag{13}$$

(which evaluate the distance from the (0,0) point using the data-spread "yardstick"). For the ADS, because of the large data spread, it is usually insignificant (see Fig.7a), but even if it were the low *V* values (0.3 in this specific case) would increase CEP by only 3% (see Fig.3).

Now we can check whether the distribution of our data is circular. We do it by calculating the *F*-statistic

$$F_s = \frac{\sigma_L^2}{\sigma_S^2} \tag{14}$$

(where σ_L is the larger standard deviation (range) and σ_S is the smaller standard deviation (azimuth deflection)) and comparing it to the critical value. In our case despite an obvious difference in the values of standard deviation for the *u* and *v* data sets (after rotation) the Fisher's *F* test with reveals that this difference (σ_L is $1.4 \approx \sqrt{1.98}$ times larger than σ_S) is insignificant (compared to the critical value of $F_{0.02,15,15} = 2.86$, where 15=*n*-1 defines the DF for numerator and denominator), i.e. in our case we can be 98% confident that distribution is circular. Hence, we may apply a generic formula for CEP applicable to CND

$$CEP = 1.1774\frac{\sigma_S + \sigma_L}{2} = 0.5887\sigma_S + 0.5887\sigma_L \tag{15}$$

Obviously, CEP by itself is not the entire story, - a confidence interval (CI) should be calculated and reported along with CEP. Specifically, the upper confidence limit (UCL) for the one-sided CI can be calculated using

$$CEP_{UCL_{(1-\alpha)\%}} = CEP \sqrt{\frac{(1+K^2)(n-1)}{\chi^2_{\{1-\alpha, \text{int}[(1+K^2)(n-1)]\}}}} \qquad (16)$$

where $K = \dfrac{\sigma_S}{\sigma_L} < 1$, n is the number of data points and $\text{int}\left[(1+K^2)(n-1)\right]$ is the integer part of $(1+K^2)(n-1)$ representing the DF to compute the χ^2 (chi-square) value for the appropriate confidence level (1-α). In the case of two-sided CI the lower and upper limits are computed as

$$CEP_{LCL_{(1-\alpha)\%}} = CEP \sqrt{\frac{(1+K^2)(n-1)}{\chi^2_{\{\alpha/2, \text{int}[(1+K^2)(n-1)]\}}}} \,, \quad CEP_{UCL_{(1-\alpha)\%}} = CEP \sqrt{\frac{(1+K^2)(n-1)}{\chi^2_{\{1-\alpha/2, \text{int}[(1+K^2)(n-1)]\}}}} \qquad (17)$$

In our case $CEP = 374m$ and $CEP_{UCL_{90}} = 493m$ as shown in Fig.7b.

What if we do not have the *x-y* data set to begin with, but are rather given the radial miss distance values? Well, in this case the Circular Error Average (CEA) (aka Mean Radial Error), still applicable for CND in the form of Eq.(4), can be computed as

$$CEA = \int_0^\infty \frac{r^2}{\sigma^2} e^{-r^2/2\sigma^2} dr = \sigma \sqrt{\frac{\pi}{2}} \qquad (18)$$

Since CEP=$\sqrt{2\ln 2}\sigma$ (see Eq.(7)), it can be related to CEA as

$$CEP = \frac{\sqrt{2\ln 2}CEA}{\sqrt{\pi/2}} = 0.9394CEA \qquad (19)$$

Hence, the maximum likelihood unbiased estimate of CEP becomes

$$CEP_3 = 0.9394 \frac{1}{n}\sum_{i=1}^n r_i \qquad (20)$$

If you cannot assume normality, you can still estimate CEP using the median, which is also a measure of location, so that 50% of the data values are on each side of it. The Median Radial Error (MRE) is computed as

$$MRE = median(r) \qquad (21)$$

Both estimates (CEP$_3$ and MRE) are also shown in the bottom-right corner of Fig.7b. The fact that they are relatively close to the CEP estimate shown in the upper-right corner indicates that the actual distribution is really close to CND as we have formally proven it using the Kolmogorov-Smirnov test already.

Figure 8 shows a relationship between different estimates of CEP obtained for some other ADS test data. Such a behavior is quite typical, and all accuracy estimates are usually characterized by the following inequality:

$$MRE < CEP_3 < CEP_{MPI} < CEP_{DMPI} < CEP_{UCL_{(1-\alpha)\%}} \qquad (22)$$
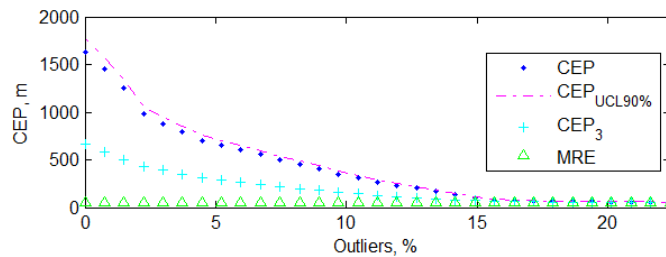

Fig. 8. Convergence of all CEP metrics versus the number of eliminated outliers.

While decreasing the size of the sample by eliminating outliers the CEP$_{MPI}$ estimate converges to that of MRE (note that MRE estimate decreases with an increase of the number of outliers as well, it is just the scale of Fig.8 prevents from seeing it). Hence, MRE may serve as a lower bound of a CEP estimate. Figure 9 shows this specific (relative) difference between CEP$_{MPI}$ and MRE that correlates with data in Fig.8. This difference can probably serve as an implicit indicator of the number of outliers in test data. In this specific case, when the number of outliers reaches about 21% the relative difference between two estimates becomes less than 15%. Obviously, further increase of the number of outliers leads to even closer match between CEP$_{MPI}$ and MRE, however there is a danger of increasing system's operational effectiveness (in the terms of OT&E) at the expense of operational suitability. To this end,

Fig.10 shows a weighted sum of a normalized CEP_{MPI} and the number of outliers this CEP estimate was computed without. For this specific case it is clear that going beyond ~21% of outliers is not rational.
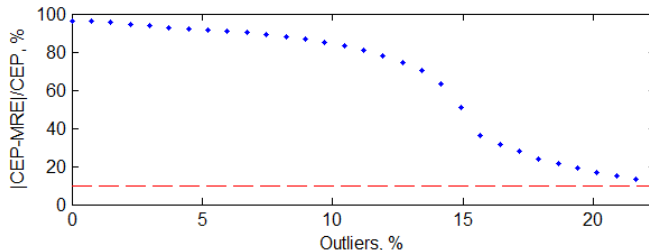

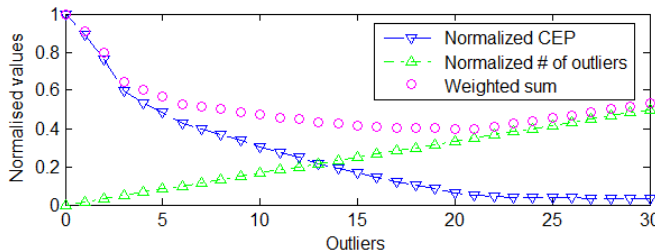Fig. 9. Relative error between CEP_{MPI} and MRE.

Fig. 10. Effectiveness versus suitability.

To conclude this section let us address one more issue. What if the F statistic (Eq.(14)) turns our to be larger than the critical value indicating that we do not have a CND? In this case (BND) we may still utilize the CEP concept, which means exactly the same - the radius of a circle encompassing 50% of data (Fig.11). The only difference is that instead of Eq.(15) we would need to use

$$CEP = 0.6183\sigma_S + 0.5619\sigma_L \qquad (23)$$

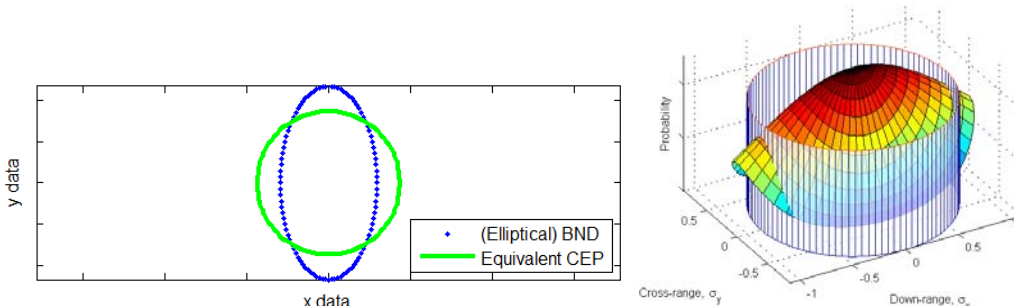(derivation of this equation is addressed in Addendum B).

Fig. 11. Graphical representation of CEP_{MPI} in the case of non-circular distribution.

Now that the approach to estimate an accuracy of self-guided ADSs has been formalized let us try to apply it to establish the overall trends in precision airdrop.

III. Trends in Precision Airdrop Accuracy

In 2001-2009 several major (PATCAD) demonstrations took place within in the DoD Joint Precision Airdrop System (JPADS) program.[10] This program involved a family of different-weight self-guided ADSs utilizing different (proprietary) GNC paradigms. Figures 12 and 13 represent statistical analysis of miss distance data obtained during four of such events.[11] The methodology for processing test data was the same as established in Section II. (Note, the axis names, down- and cross-range, in these and the following figures are used quite loosely.)

As seen from Figs.12,13, from the standpoint of statistics there is a lot of similarities between test data obtained at all four events. Elimination of the essential number of outliers brings miss distance distributions close to normal (the box plots characterize reduced data sets after exclusion of most obvious outliers). The overall reliability of the systems becomes better, so that the number of outliers decreases from 38% down to about 25% (among all ~10 ADSs demonstrated at each event). The V value happens to be small for the first three events and relatively large (still below 0.5) for the fourth event. The latter was caused partly because of reduced CEP, but also because of the strong winds (on some occasions of the order of the forward speed of ADS). However, the bias happens to be not

statistically significant for any data set. All distributions are close to circular, which is probably caused by the specific features of GNC algorithms typical for most of ADSs.
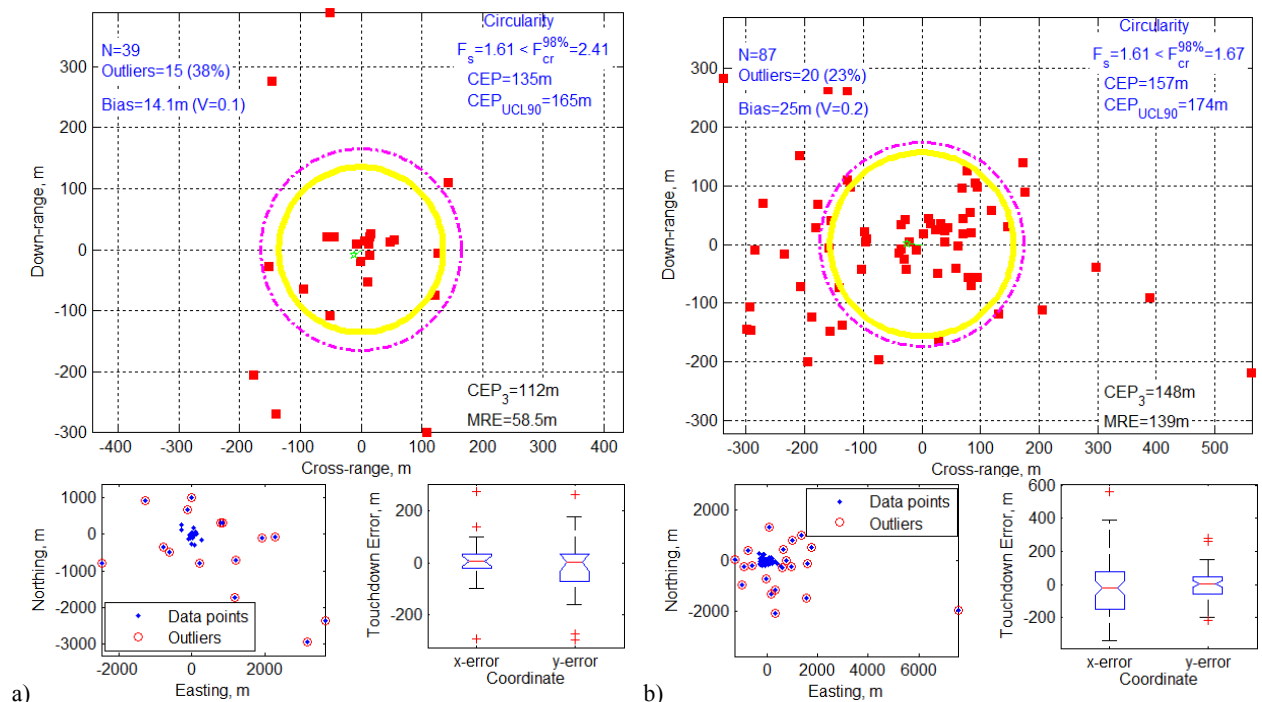

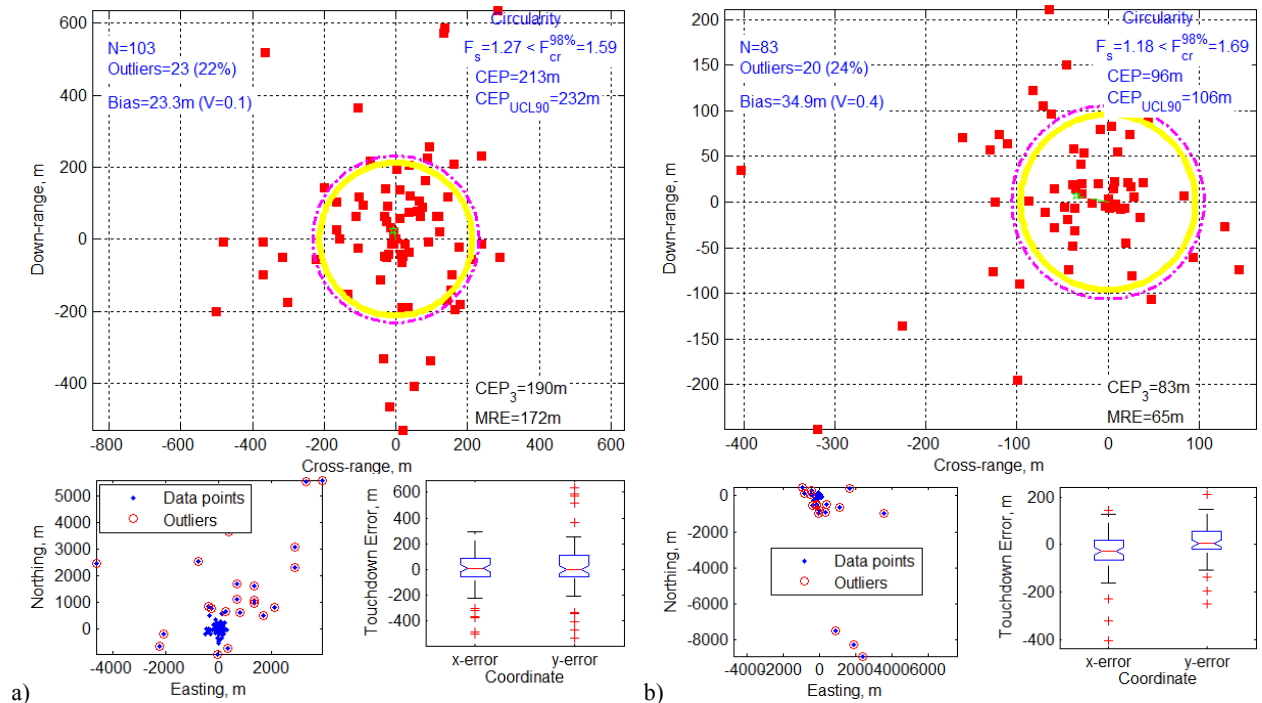Fig. 12. Overall performance at PATCAD 2003 (a) and PATCAD 2005 (b).

Fig. 13. Overall performance at PATCAD 2007 (a) and PATCAD 2009 (b).

Figure 14 features the MRE estimates obtained by consequent elimination of more and more worst data points for each of the five PATCAD events computed according to Eq.(21) (again, MRE represents a lower bound of a CEP estimate as explained in Section II). Horizontal axis shows the percentage of test data that was considered for MRE computation. This figure clearly indicates the overall improvement of aerial payload delivery accuracy in the course of eight years no matter how many points one decides to eliminate due to the different reasons.

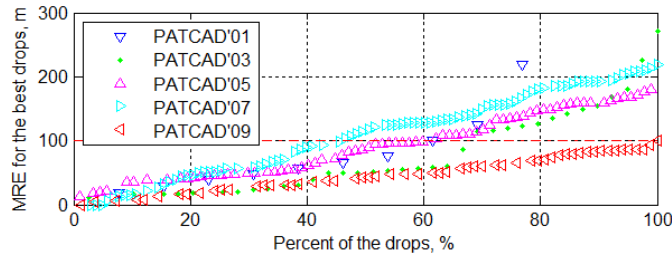American Institute of Aeronautics and Astronautics

Fig. 14. PATCAD 2001-2009 performance.

Figure 15 represents miss distances normalized by the corresponding MRE, so that all dependences intersect a (50%,1MRE) point. If data were distributed according to CND, 99.8% of all data points would reside within 3 MRE (CEP). However, it is not the case. O average, about 25% of data fall outside the 3MRE limit. Interestingly enough this percentage is about the same as the percentage of accepted outliers (see Figs.12,13). Another observation is that for PATCAD'01 the overall distribution happens to be much closer to that of CND. That suggests that it is probably basic ADS flight performance along with GNC paradigm that affect a touchdown accuracy the most because 30% of the data points for PATCAD'01 belonged to a parachute-based ADS with a GNC scheme cardinally different from those of parafoil-based ADSs. To investigate this issue a little bit further next section considers several different ADSs separately as opposed to the data points comprised of multiple systems as discussed in this section.
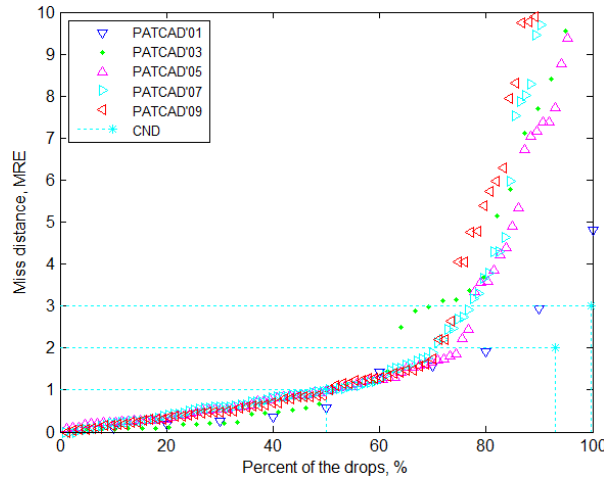

Fig. 15. Miss distance distribution (in the units of MRE).

IV.   Effects of ADS's Size and GNC Algorithms

According to JPADS classification there are several weight classes for self-guided ADSs as follows:[12]
- Medium weight (MW):   7tn - 20tn
- Light weight (LW):   2tn - 5tn
- Extra Light weight (XLW):   300kg - 1tn
- Ultra Light weight (ULW):   70kg - 300kg
- Micro Light weight (MLW):   < 70kg

Figures 16 and 17 demonstrate statistical analysis of miss distances for some typical ADSs in different weight categories. Even though in this case the data points characterize a single system as opposed to several systems at once as it was the case in Section III, all major observations are still the same. The number of outliers needed to be removed varies from 36% for more complex MW ADSs all way down to 13% for the lighter ones attesting to their maturity (operational suitability). The biases are statistically insignificant with the small values of V even for the systems with low CEP (Fig.14), the distributions are close to CND (for XLW ADS $\sigma_L = 1.07\sigma_S$).
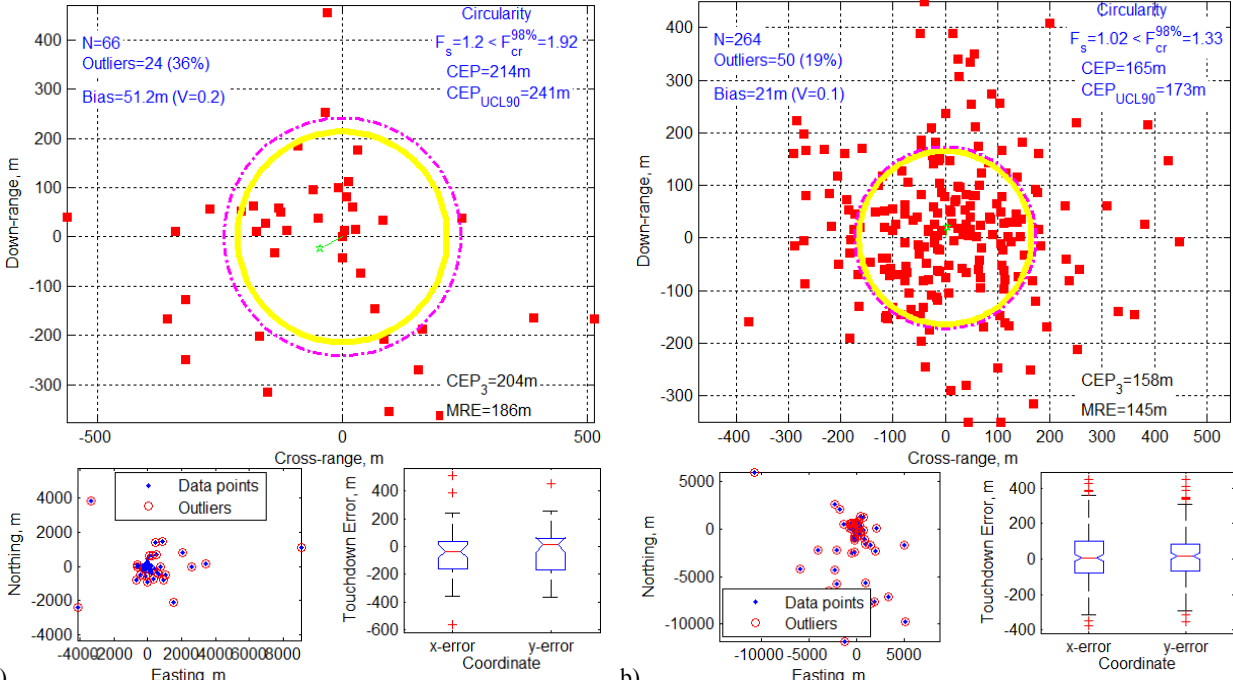
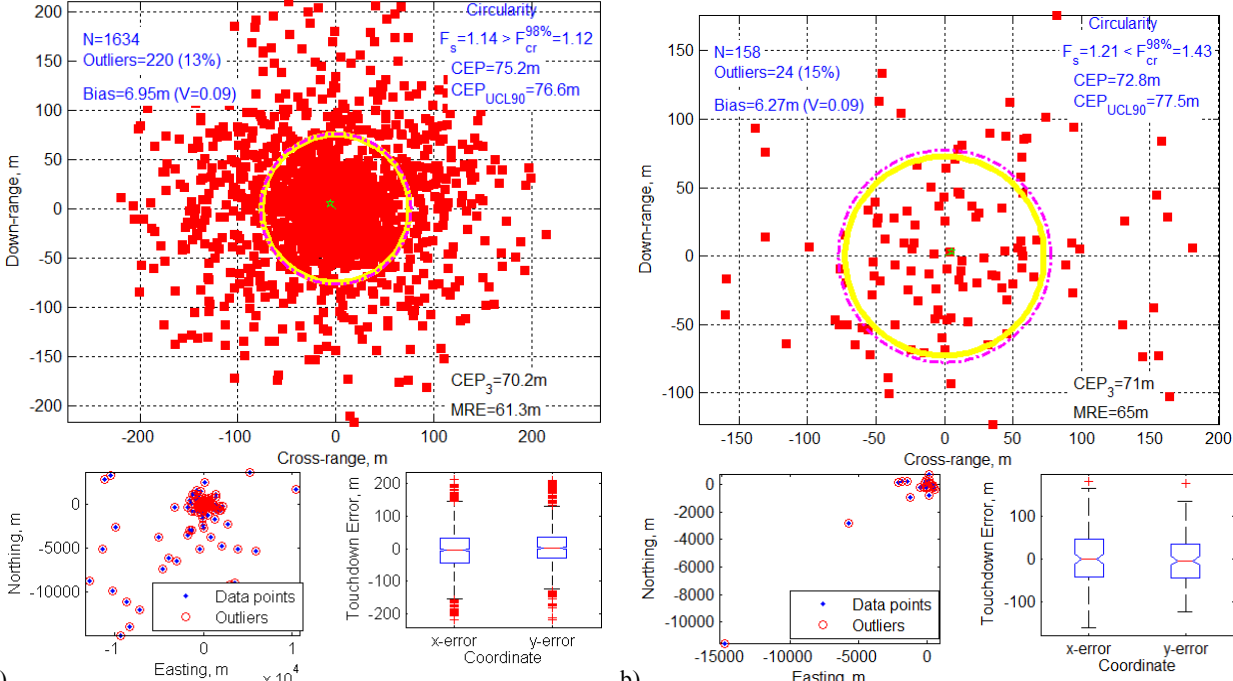Fig. 16. Typical performance of MWADS (a) and LW ADS (b).

Fig. 17. Typical performance of XLW ADS (a) and ULW ADS (b).

For comparison, Fig.18 shows statistical data for two more ULW ADSs. All observations presented above are generally valid for these two ADSs as well (with a slightly larger number of outliers, but smaller values of the CEP estimates).

Figure 19 exhibits the same type of dependencies as that of Fig.14, but for representatives of MW/LW/XLV/ULW ADSs. Again, it shows the overall trends based on the lower bound of CEP estimate. Clearly, if nothing else but ADS' weight does affect the overall performance. Weight of ADS though may have an indirect influence via a turn radius, which happens to be proportional to the value of a CEP estimate for each system.

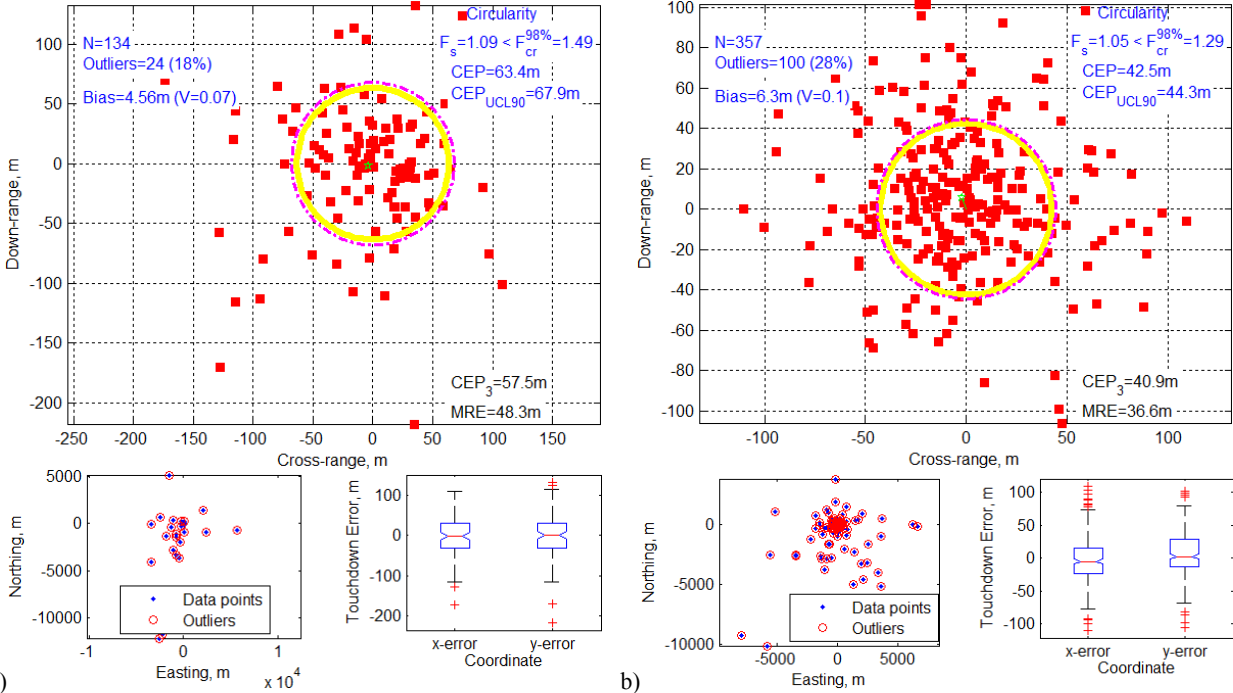American Institute of Aeronautics and Astronautics
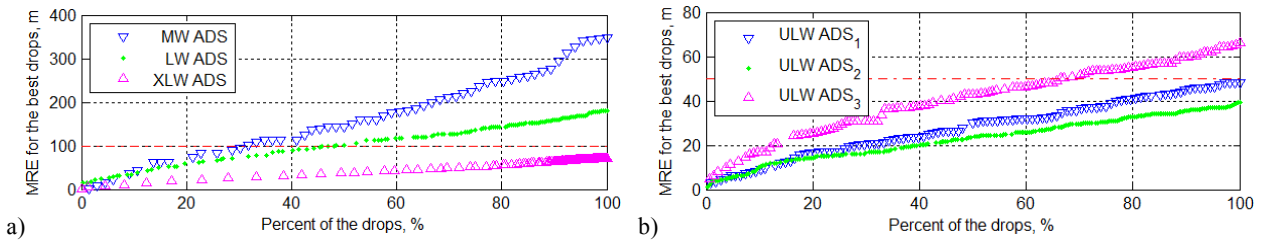
Fig. 18. Performance of two ULW ADSs.

Fig. 19. MW/LW/XLV ADSs performance (a) and ULW ADSs performance (b).

As mentioned above, if data were to follow CND the points of impact (PIs) would tend to cluster around the aim point, with most reasonably close, progressively fewer and fewer further away, and very few at long distance. To this end, Fig.20a shows actual touchdown error distributions for all systems presented in Figs.16,17a, while Fig.20b presents distributions for three different ULW ADSs shown in Figs.17b,18. As seen, in the case of self-guided ADSs it is about 20% (on average) of the drops that are farther than 3 MRE (CEP) as opposed to just 0.2% for the classical CND. What is interesting is that these three different-weight-category ADSs in Fig.20a exploit about the same guidance strategy, while three same-weight-category ADSs in Fig.20b exercise different guidance strategies! As a result three distributions of Fig.20a are much closer to each other compared to those three in Fig.20b. Hence, as it was hypothesized when observing the plots in Fig.15, the guidance strategy not only affects the overall touchdown accuracy by itself, but also causes changes in the tails of distributions making them either heavy, like ADS_2 in Fig.20, or closer to that of a classical CND (ADS_3).

V.   Outliers Distribution

While the previous sections concentrated on a proper procedure to remove outliers in order to estimate ADS's performance in terms of CEP, from the standpoint of a test planning officer these outliers represent a major interest / concern. (S)he needs to know how far these outliers may be off the 3 CEP circle around IPI, what a probability of such an event is, what distribution these outliers exhibit, and what the worst case scenario would be (estimating the largest miss distance). Toward this goal, Figs.21-25 represent the analysis of outliers that were removed to estimate CEP as shown in Figs.12,13,16-18.

The first observation is that in the most of the cases there is a strong correlation between x and y sets of data (revealed in this case by the Spearman's rho test as indicated in Table 1) resulting in the necessity to rotate the data

American Institute of Aeronautics and Astronautics

sets (again, the axis names, down- and cross-range, are used loosely). It is probably safe to attribute it to the direction of the prevailing winds (which by the way also defines the position of a release point with respect to IPI).
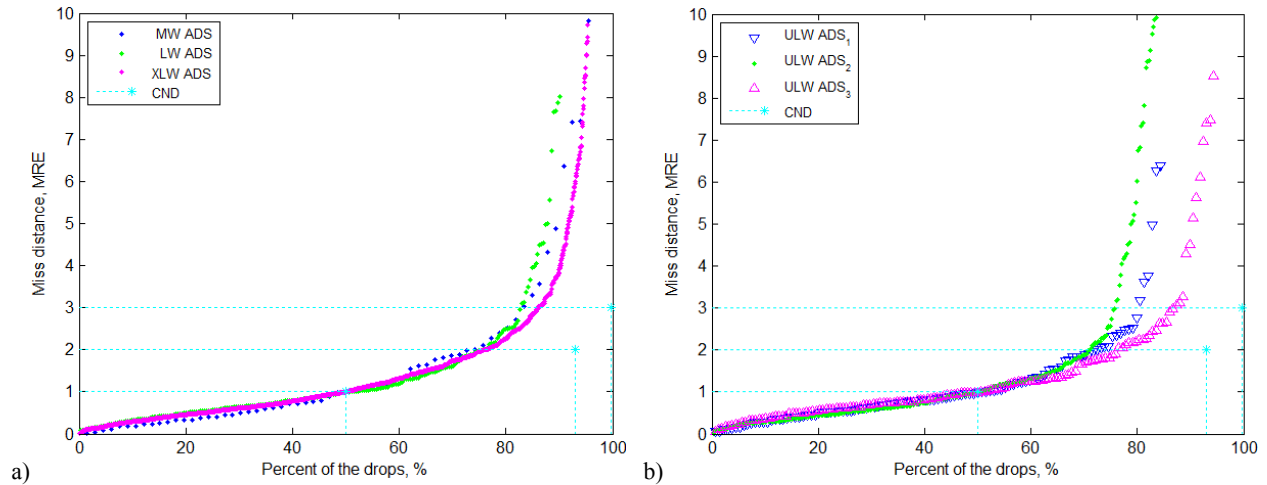

Fig. 20. Miss distance distribution (in the units of MRE) for different-weight-category ADSs (a) and the same-weight-category ADSs (b).
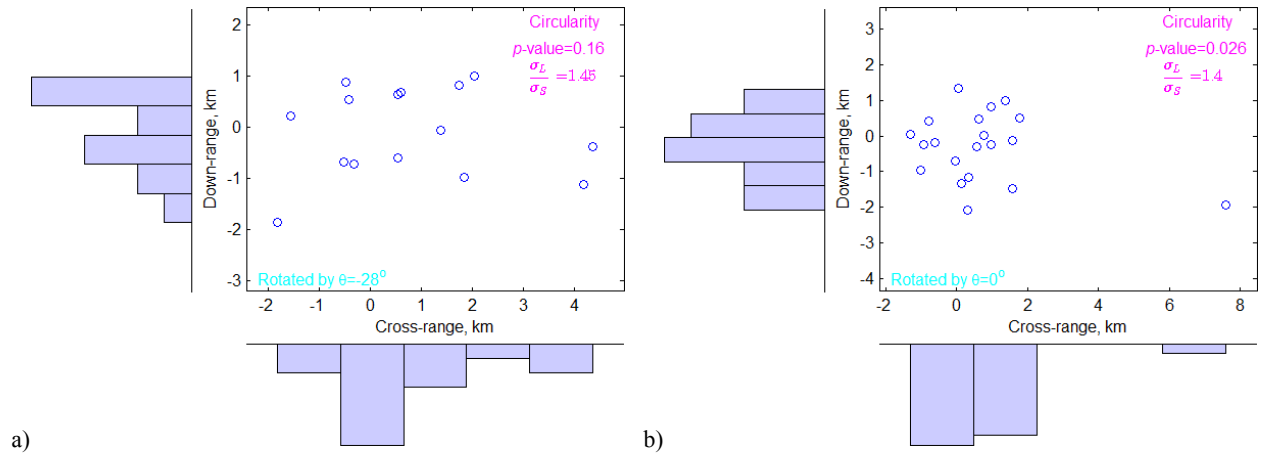

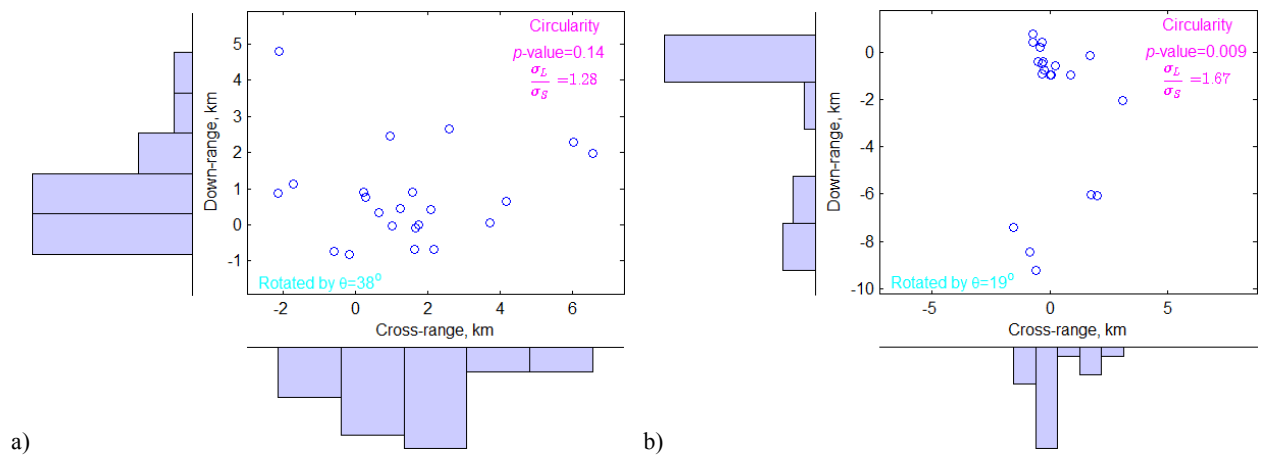Fig. 21. Outliers corresponding to data shown in Fig.12.

Fig. 22. Outliers corresponding to data shown in Fig.13.

The second observation is that some data sets contain obvious outliers that are most likely caused by the complete or partial failure to deploy a canopy (see Figs. 21b, 22b, 23a, 24b, 25b). Another reason may be that the IPI coordinates were not entered into the system correctly, so it tries to steer to the point which is miles away from the actual IPI. Both events happen quite rarely (especially for mature ADSs) and the only way to account for them is

American Institute of Aeronautics and Astronautics

to compute a full-fledged safety fan based on parameters of a release point and ADS' characteristics (glide ratio), exactly how the Safety Fans GUI does it.[1,2] If these extreme outliers are eliminated from the further analysis then we usually have a distribution featuring a slightly larger dispersion of data along one axis of the correlation compared to that on another axis. If characterized by the standard deviation (which may not be exactly the right thing to use in this case), on the average we have about 25% difference (which as explained in the previous section is most likely caused by the essence of GNC algorithms). It is interesting though that running a formal non-parametric Siegel-Turkey test (see Table 1) does not necessarily treats these differences as being statistically significant (see Figs. 21a, 22a, 23a, 24b, 25b). On the contrary, the outlier distributions may be though as close to circular.
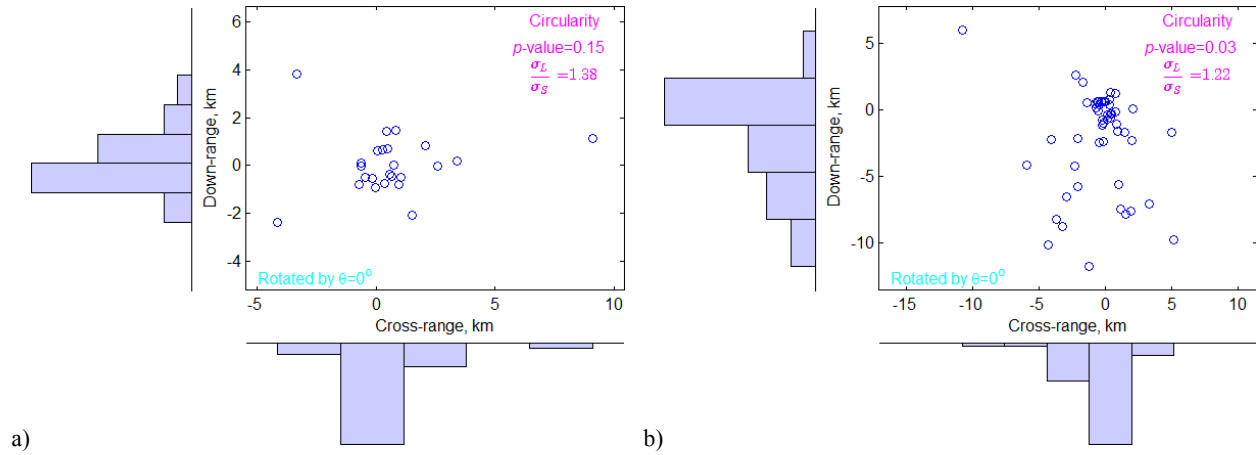

a)   b)
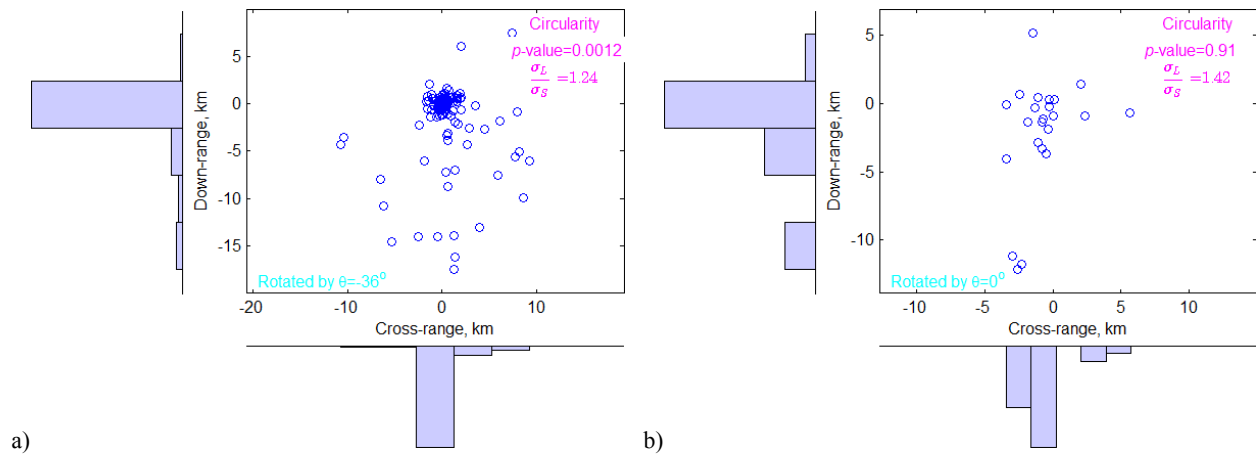
Fig. 23. Outliers corresponding to data shown in Fig.16.

a)   b)

Fig. 24. Outliers corresponding to data shown in Fig.17.

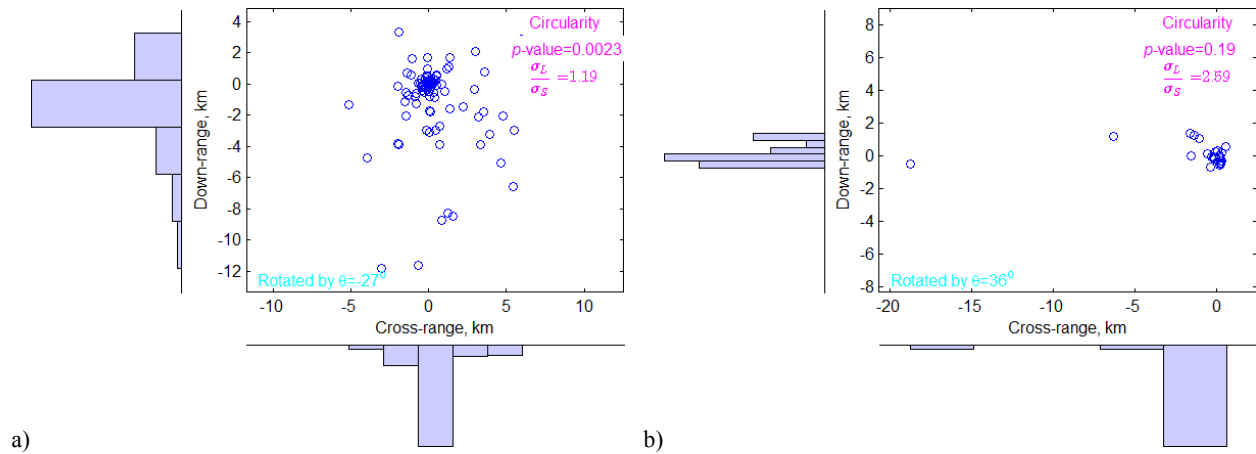a)   b)

Fig. 25. Outliers corresponding to data shown in Fig.18.

American Institute of Aeronautics and Astronautics

VI. Conclusion

The paper suggested a unified methodology for evaluating touchdown error performance of self-guided aerial payload delivery systems adapted from that of the science of ballistics. It showed the differences with the latter and established a relationship between different estimates of CEP depending on the number of outliers. Using the developed methodology performance of a variety of ADSs was evaluated to show that: a) easily obtained and robust MRE may serve as a lower bound of a CEP estimate; b) touchdown error distribution features heavy tails so that the chance of ADS landing beyond a 3 MRE circle around IPI is about two orders of magnitude higher than it would be in the case of classical CND; c) elimination of outliers resigning in those heavy tails brings touchdown error distribution closer to CND, meaning that standard deviations for *x* and *y* data are about the same and bias being statistically insignificant. The detailed analysis also revealed a strong dependence of ADS's size (weight) and GNC strategy on the CEP value. It is also argued that a guidance strategy has a strong effect on the miss distance distribution in general, being in control of the tails of touchdown error distribution. Finally, the outlier distributions (for not fully failed, properly operating systems) may be thought of as being close to circular. As far as DT and OT planning, the Safety Fans GUI is now being updated to compute a possible PIs footprint more accurately with certain probabilities. That is accomplished by accounting for the size (weight category) of ADS (its turn radius), its maturity and essence of guidance strategy.

References

[1]Corley, M.S., and Yakimenko, O.A., "Computation of the Safety Fans for Multistage Aerodelivery Systems," *Proceedings of the 20th AIAA Aerodynamic Decelerator Systems Technology Conference and Seminar*, Seattle, WA, May 4-7 2009.

[2]Mulloy, C.C., Tiaden, R.D, and Yakimenko, O.A., "The 2nd Generation of Safety Fans GUI," *Proceedings of the 21st AIAA Aerodynamic Decelerator Systems Technology Conference*, Dublin, Ireland, May 23-26, 2011.

[3]Giadrosich, D., *Operations Research Analysis in Test and Evaluation*, AIAA Educational Series, Reston, VA, 1995.

[4]Driels, M., *Weaponeering: Conventional Weapon Systems Effectiveness*, AIAA Educational Series, Reston, VA, 2004.

[5]Hayter, A.J., *Probability and Statistics for Engineers and Scientists*, 4th Edition, Duxbury Press, 2012.

[6]Spearman, C., "The Proof and Measurement of Association Between Two Things," *American Journal of Psychology*, 15(**1**), 1904, pp.72–101.

[7]Lilliefors, H., "On the Kolmogorov-Smirnov Test for Normality with Mean and Variance Unknown," *Journal of the American Statistical Association*, 62(**318**), 1967, pp.399–402.

[8]Corder, G.W, Foreman, D.I., *Nonparametric Statistics for Non-Statisticians: A Step-by-Step Approach*. Wiley, Hoboken, NJ, 2009.

[9]Wilcoxon, F., "Individual Comparisons by Ranking Methods," *Biometrics Bulletin*, 1(**7**): 1945, pp.80–83.

[10]Benney, R., McGrath, J., McHugh, J., Meloni, A., Noetscher, G., Tavan, S., Patel, S., "DOD JPADS Programs Overview & NATO Activities," *Proceedings of the 19th AIAA Aerodynamic Decelerator Systems Technology Conference and Seminar*, Williamsburg, VA, May 21-24, 2007.

[11]Precision Airdrop Technology Conference and Demonstration, Final Report, U.S. Army RDECOM, Natick, MA, 2001, 2003, 2005, 2007, 2009.

[12]Benney, R., Meloni, A., Henry, M., Lafond, K., Cook, G., Patel, S., and Goodell, L, "Joint Medical Distance Support and Evaluation (JMDSE) Joint Capability Technology Demonstration (JCTD) & Joint Precision Air Delivery Systems (JPADS)," *Proceedings of the Special Operations Forces Industry Conference*, Tampa, FL, June 2-4, 2009.

In order to compute CEP_{DMI} we need to start with CND that has a bias (for the purpose of derivation of the correct formula we may assume that this bias is along one of the axes, say x-axis). Then, Eq.(4) becomes

$$p(x,y) = \frac{1}{2\pi\sigma^2} e^{-\frac{(x-Bias)^2+y^2}{2\sigma^2}} \tag{A1}$$

Introducing $x = r\cos(\varphi)$ and $y = r\sin(\varphi)$ allows representing the probability of radius r (CEP_{DMI}) being less than some value a as

$$P(r \le a) = \frac{1}{2\pi\sigma^2} \int_0^a \int_0^{2\pi} re^{-\frac{r^2-2rBias\cos(\varphi)+Bias^2}{2\sigma^2}} \, dr d\varphi \tag{A2}$$

(which is similar to Eq.(5)). Now, recalling Eq.(7) leads to

$$P(r \le a) = \frac{2\ln 2}{\pi CEP_{MPI}^2} \int_0^a \int_0^{2\pi} re^{-\ln 2\frac{r^2-2rBias\cos(\varphi)+Bias^2}{CEP_{MPI}^2}} \, dr d\varphi \tag{A3}$$

Finally, introducing $V = \frac{Bias}{CEP_{MPI}}$ and $k_{Bias} = \frac{CEP_{DMPI}}{CEP_{MPI}}$ allows rewriting Eq.(A3) as

$$P(r \le a) = \frac{\ln 2}{\pi} \int_0^{k_{Bias}} \int_0^{2\pi} \bar{r}e^{-\ln 2(\bar{r}^2-2\bar{r}V\cos(\varphi)+V^2)} \, d\bar{r}d\varphi \tag{A4}$$

Since we want this probability P to be equal to 0.5 (the definition of CEP_{DMPI}), we finally get

$$0.5 = \frac{\ln 2}{\pi} \int_0^{k_{Bias}} \int_0^{2\pi} \bar{r}e^{-\ln 2(\bar{r}^2-2\bar{r}V\cos(\varphi)+V^2)} \, d\bar{r}d\varphi \tag{A5}$$

Unfortunately, Eq.(A5) has no analytical solution (with respect to k_{Bias}), so we have to solve it numerically for a set of V values. Figure A1 represents such numerical solutions obtained for $V \in [0; 2.2]$ along with a cubic regression with respect to parameter V. This regression, known as RAND 234 formula, is widely used ballistics. Residuals for this formula are of the order of 10^{-3}.
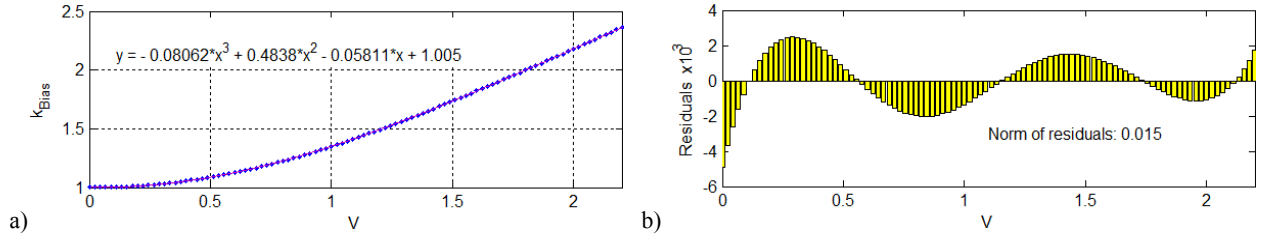

a)   b)

Fig. A1. Numerical solutions of Eq.(A5) and cubic regression $k_{Bias} = k_{Bias}(V)$ for $V \in [0; 2.2]$. and corresponding residuals (b).

Because of the wide dispersion of the touchdown points for self-guided ADSs the V ratio happens to be much smaller compared to that in ballistics. For mature ADSs it is less than 0.1, for new systems it may be around 0.5. Figure A2 shows solutions of Eq.(A5) for another interval, $V \in [0; 0.5]$, along with more accurate cubic regression for this range of V. Figure 3 in the beginning of this paper represents the same data but features even simpler, quadratic regression that has the norm of residuals of the order of $2 \cdot 10^{-4}$.
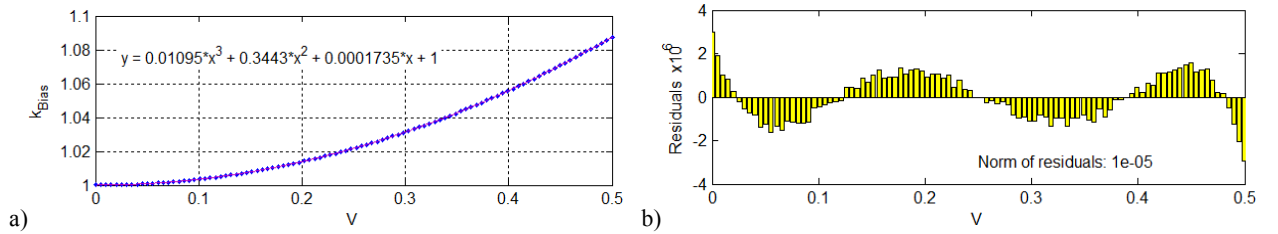

a)   b)

Fig. A2. Numerical solutions of Eq.(A5) and a cubic regression $k_{Bias} = k_{Bias}(V)$ for $V \in [0; 0.5]$ (a) with corresponding residuals (b).

Addendum B. Computation of CEP$_{MPI}$ for Non-Circular Distribution.

In the case when $\sigma_x \neq \sigma_y$ (let us assume no bias, $\mu_x = \mu_y = 0$, and no correlation, $\rho = 0$), BND (Eq.(1)) reduces to the elliptical distribution

$$p(x,y) = \frac{1}{2\pi\sigma_x\sigma_y} e^{-\frac{x^2}{2\sigma_x^2}-\frac{y^2}{2\sigma_y^2}} \tag{B1}$$

In this case, the probability of radius r being less than some value a is computed as

$$P(r \leq a) = \iint_S \frac{1}{2\pi\sigma_x\sigma_y} e^{-\frac{x^2}{2\sigma_x^2}-\frac{y^2}{2\sigma_y^2}} dxdy = \int_0^r \int_0^{2\pi} \frac{1}{2\pi\sigma_x\sigma_y} e^{-\frac{(r\cos\varphi)^2}{2\sigma_x^2}-\frac{(r\sin\varphi)^2}{2\sigma_y^2}} r d\varphi dr \tag{B2}$$

By equating this expression to 0.5 and solving it numerically we may establish a dependence of CEP from the ratio $K = \dfrac{\sigma_S}{\sigma_L}$. These dependences are shown in Fig.B1 for two ranges, $K \in [0.3;1]$ and $K < 0.3$, along with the linear and quadratic regressions, respectively. As seen from Fig.B1, for these two ranges the best fit yields the following estimates:

$$K \in [0.3;1]: \qquad CEP_{MPI} = 0.6183\sigma_S + 0.5619\sigma_L \quad \text{(see Eq.(23))} \tag{B3}$$

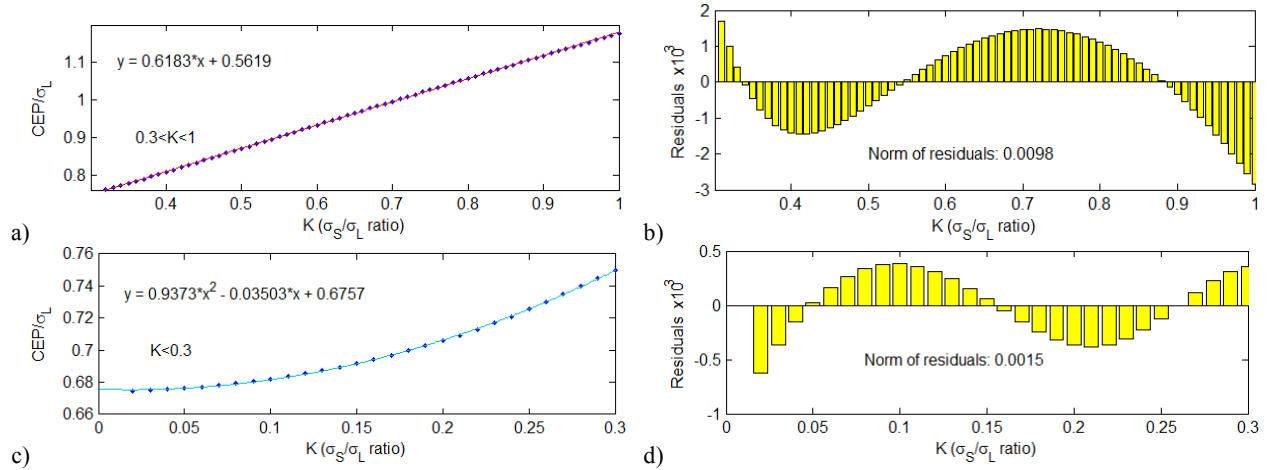$$K \leq 0.3: \qquad CEP_{MPI} = (0.9373K - 0.0350)\sigma_S + 0.6757\sigma_L \tag{B4}$$

Fig. B1. Numerical solutions of Eq.(B2) for two ranges, $K \in [0.3;1]$ (a) and $K < 0.3$ (c), with regressions and corresponding residuals (b and d, respectively).